European Journal of Inorganic Chemistry

Supporting Information

Exploration of Metal-Metal Charge Transfer (MMCT) and its Effect in Generating New Colored Compounds in Mixed Metal Oxides

Indrani. G. Shanmugapriya, Supratik Mukherjee, Alfonso Muñoz, Ganapathy Vaitheeswaran,* and Srinivasan Natarajan*

Figures and table Captions for Electronic Supporting Information

Characterizations

Table S1. Crystallographic information about $Zn_3V_2O_8$.

Table S2: The reaction condition for prepared oxide samples.

Figure S1: Color of $Zn_{3-x}M_xV_2O_8$ (M= Co, Ni, Cu) powder samples under day light.

Figure S2: PXRD patterns of $Zn_{3-x}M_xV_2O_8$ (M= Co, Ni, Cu) prepared vanadate compounds.

Figure S3. Rietveld refinement and Crystallographic parameters generated from the Rietveld refinement for $Zn_{3-x}M_xV_2O_8$ (M= Co, Ni, Cu).

Figure S4. Tanabe–Sugano diagrams of (a) d^7 (b) d^8 and orgel diagram of (c) d^9 configurations.

Figure S5. Optical absorption (UV/Vis) spectra of $Zn_{3-x}M_xV_2O_8$ (M= Co, Ni, Cu) prepared vanadate compounds.

Figure S6: SEM-EDX spectra of $Zn_{3-x}M_xV_2O_8$ (M= Co, Ni, Cu).

Figure S7: PXRD patterns of $Zn_{3-X}M_xP_2O_8$ (M= Co, Ni) prepared Phosphate compounds.

Figure S8. Rietveld refinement and crystallographic parameters generated from the Rietveld refinement for $Zn_{3-x}M_xP_2O_8$(M=Co, Ni).

Figure S9: The crystal structure and crystallographic information of $Zn_2MgP_2O_8$ (γ-$Zn_3P_2O_8$).

Figure S10: PXRD patterns of $Zn_{3-X}M_xP_2O_8$ (M= Cu) prepared Phosphate compounds.

Figure S11. Crystal structure and crystallographic information of α-$Zn_3P_2O_8$.

Figure S12. Color of $Zn_{3-x}M_xP_2O_8$ (M= Co, Ni, Cu) powder samples under day light.

Figure S13: Correlation diagram for Co^{2+} with symmetries C_{4v}, D_{3h} (Co), T_d (Co) and O_h (Co).

Figure S14: Tanabe Sugano diagram for trigonal bipyramidal geometry of Co^{2+} and Ni^{2+} ions.

Figure S15. Optical absorption (UV/Vis) spectra of the $Zn_{3-x}Cu_xP_2O_8$ ($0 < x \leq 0.1$).

Figure S16. SEM-EDX spectra of $Zn_{3-x}M_xP_2O_8$(M=Co, Ni).

Figure S17. Crystal structure and crystallographic information of Co_2TiO_4 and Co_2SnO_4.

Figure S18: PXRD Pattern of $Zn_{2-x}Co_xTiO_4$ doped samples.

Figure S19: PXRD Pattern of $Zn_{2-x}Co_xSnO_4$ doped samples.

Figure S20. The color of $Zn_{2-x}Co_xAO_4$ (A=Ti, Sn) powder samples under day light.

Figure S21. Orgel and Tanabe Sugano diagram for Co^{2+} in both octahedral and tetrahedral geometry.

Figure S22. NIR reflectivity of $Zn_{3-x}M_xV_2O_8$ (M= Co, Ni, Cu).

Figure S23. NIR reflectivity of $Zn_{3-x}M_xP_2O_8$(M= Co, Ni, Cu).

Figure S24. CIE 1931 chromaticity diagram and CIE coordinates for $Zn_{3-x}M_xA_2O_8$(M= Co, Ni, Cu). (A = V, P).

Figure S25. CIE 1931 plot, color coordinates and CIE coordinates of $Zn_{2-x}Co_xAO_4$ (A=Ti, Sn) powder samples.

References

Characterizations:

All the prepared oxides were characterized by PXRD, scanning electron microscopy (SEM) with energy-dispersive X-ray spectroscopy (EDX). PXRD patterns were recorded using Panalytical EMPYREAN diffractometer (Ni-filtered Cu Kα radiation, λ = 1.5406 Å). PXRD data for the Rietveld refinement of the structures were collected at room temperature in the 2θ range 5−120° with a step size of 0.02° and step duration 50 s. About 100 mg of the powdered samples were tightly packed in a rectangular sample holder (1 X 2 cm) for recording the PXRD data. The structure of representative members were refined from PXRD data using the program **GSAS** (General Structure Analysis System)- **EXPGUI** (Graphical User Interface)[1]. A second order shifted Chebyschev polynomial for the background, lattice and atomic parameters, scale factors, background (Fourier polynomial background function), pseudo-Voigt profile functions (U, V, W, and X), and isothermal temperature factors (U_{iso}) were used in refinement. Thermal parameters were constrained to be the same for different atoms occupying the same sites[2] (Zn and M^{II}). The diffuse reflectance spectra for all powdered samples were recorded on Perkin−Elmer Lambda 950 UV/vis double beam spectrometer over the spectral region of 200−2500 nm. The diffuse reflectance data were converted to absorbance data employing the Kubelka−Munk[3] function by using the equation (1)

$$F(R) = \frac{1-R2}{2R} = \frac{\alpha}{S} \quad (1)$$

in which R is the reflectance, α is absorptivity, and S is the scattering factor. The optical band gaps were calculated from Tauc plots.[4] The Tauc relation (2) is

$$\alpha h\nu = A(h\nu - Eg)n \quad (2)$$

where α is absorption coefficient, A is a constant called the band tailing parameter, and n is the power factor of the transition mode. The Plot of $(\alpha h\nu)^{(1/n)}$ versus the photon energy (hν) gives a straight line in a certain region. The extrapolation of this straight line intercepts the (hν)-axis to give the value of the optical band gap (E_g). NIR reflectance in the λ = 500−2500 nm range at room temperature were collected by using the same instrument. For characterization of pigment quality of the samples, the CIE 1931 chromaticity[5] coordinates in the λ = 380−750 nm range were collected by using the same instrument. The CIE 1931 chromaticity coordinates were determined by using the gocie.exe program[6]. SEM images and EDX[7] data were recorded on a FEI ESEM Quanta 200 scanning electron microscope.

Table S1. Crystallographic information about $Zn_3V_2O_8$

Crystal system	Orthorhombic
Space group	*C* m c a (64)
Unit cell dimensions	*a* = 6.088(3) Å; b=11.489(3); c=8.280(3) Å
Cell volume	579.14 Å^3
Z	4

Atom	Oxidation state	Wyck symbol	X	Y	Z	SOF
Zn	+2	4 a	0	0	0	1
Zn	+2	8 e	0.25	0.1359(2)	0.25	1
V	+5	8 f	0	0.3780(2)	0.1228(3)	1
O	-2	8 f	0	0.249(1)	0.232(1)	1
O	-2	8 f	0	0.002(1)	0.245(1)	1
O	-2	16 g	0.2286(8)	0.3814(8)	-0.005(1)	1

Table S2: The reaction condition for prepared samples

SI. No	Compound	Temperature (°C) / Time (h)	Heating Rate (°C/hr)
1	$Zn_{3-x}M_xV_2O_8$ (M= Co, Ni, Cu) $(0.05 \leq x \leq 0.5)$	650/12; 650/12	130
2	$Zn_{3-x}M_XP_2O_8$ (M=Co,Ni) $(0.25 \leq x \leq 0.5)$	720/10	300
3	$Zn_{3-x}M_XP_2O_8$ (M=Cu) $(0.05 \leq x \leq 0.1)$	700/12	150
4	$Zn_{2-x}M_XSnO_4$ (M=Co) $(0 \leq x \leq 2)$	1000/10	300
5	$Zn_{2-x}M_XTiO_4$(M=Co) $(0 \leq x \leq 2)$	900/10	300

Color of the doped sample under day light

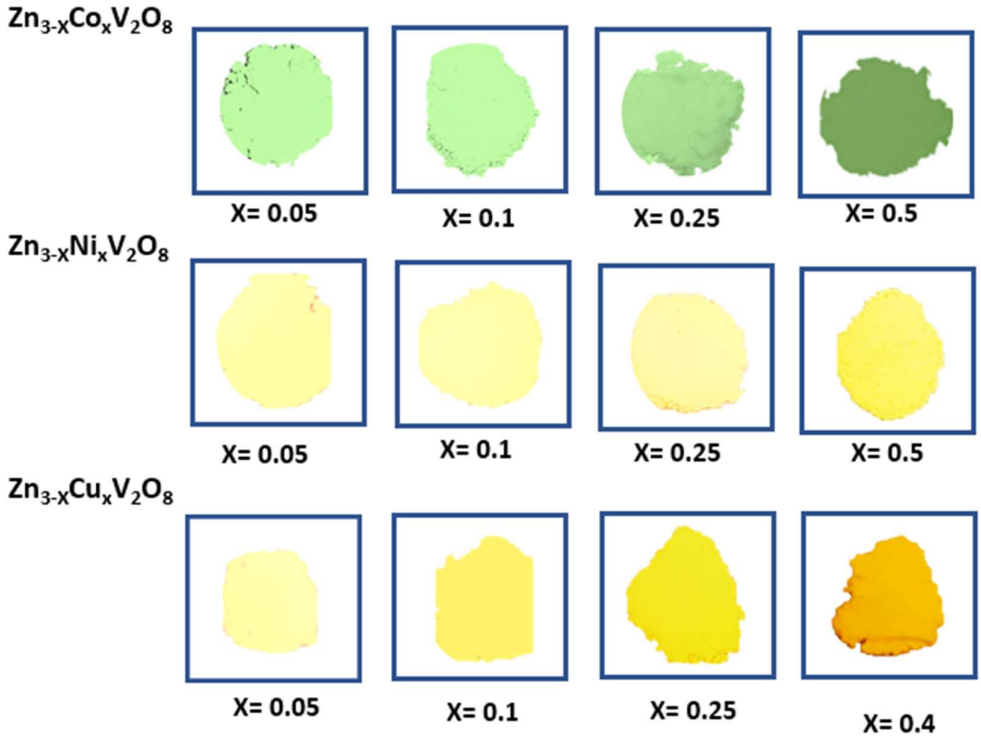

Figure S1. Color of $Zn_{3-x}M_xV_2O_8$ (M=Co, Ni, Cu) powder samples under day light.

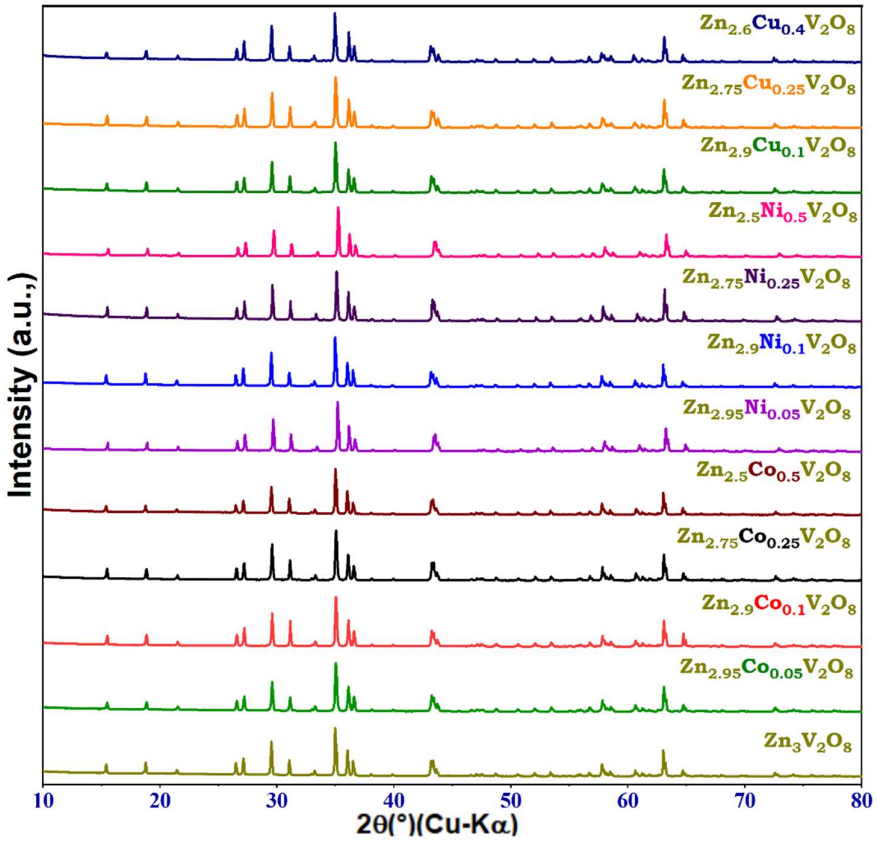

Figure S2: PXRD patterns of $Zn_{3-x}M_xV_2O_8$ (M= Co, Ni, Cu) prepared vanadate compounds.

Rietveld refinement for Co^{2+} substituted vanadate compound

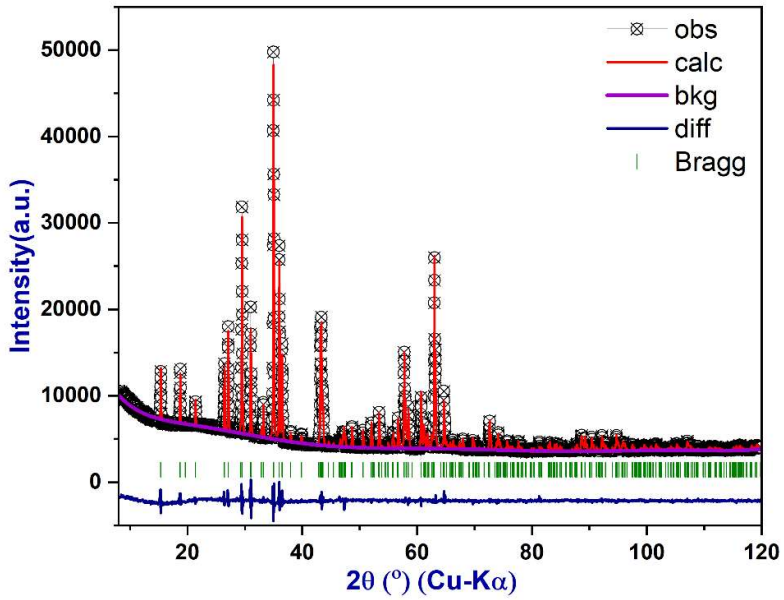

Crystallographic parameters for $Zn_{2.5}Co_{0.5}V_2O_8$ compound generated from the Rietveld refinement of the PXRD data.

Atom	Wyck. Symbol	x/a	y/b	z/c	Site Sym	Frac	U [Å²]
Zn2/Co1	8 e	0.25000	0.13990	0.25000	2(y)	0.666/0.334	0.00084
Zn1	4 a	0.0	0.0	0.0	2/m(x)	1	0.02819
V1	8 f	0.00000	0.37515	0.12518	m(x)	1.0	0.00267
O1	8 f	0.00000	0.26240	0.23511	m(x)	1.0	0.03280
O2	8 f	0.00000	0.99202	0.26093	m(x)	1.0	0.05032
O3	16 g	0.22482	0.37373	0.00748	1	1.0	0.00570

Space Group: *C*mca (64); a=6.09845(8)Å; b=11.52118(15)Å; c=8.29992(10)Å ;

α=β=γ= 90;Z=4; V=583.166Å^3.

Reliability Factors: Rp = 2.20%, Rwp = 3.02%, $\chi 2$ = 4.96.

Bond Lengths (Å): Zn1/Co1-O : 2.1393Å (Avg.); Zn2-O:2.1920Å (Avg.); V-O: 1.6551Å (Avg.)

Δ= 1.5667 [Zn2/Co1]; Δ= 1.5667 [Zn1]: 0.193

Δ is the polyhedral distortion parameter defined by $\Delta = 1/N \sum [\{(r_i - r)/r\}^2]10^3$; where

N is the number of bonds and r_i and r are individual and average bond lengths, respectively

Rietveld refinement for Ni^{2+} substituted vanadate compound

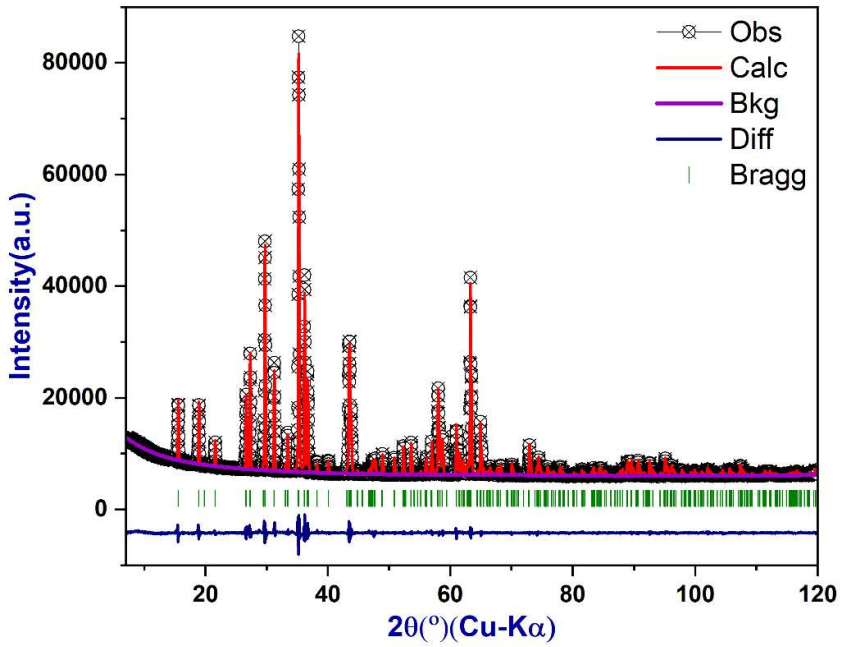

Crystallographic parameters for $(Ni_{0.5}Zn_{2.5})\ V_2O_8$ compound generated from the Rietveld refinement of the PXRD data.

Atom	Wyck. Symbol	x/a	y/b	z/c	Site Sym	Frac	U [Å²]
Zn2/Ni1	8 e	0.25000	0.13664	0.25000	2(y)	0.667/0.334	0.0086
Zn1	4 a	0.0	0.0	0.0	2/m(x)	1	0.0182
V1	8 f	0.00000	0.37576	0.12526	m(x)	1.0	0.0055
O1	8 f	0.000000	0.256138	0.229509	m(x)	1.0	0.0088
O2	8 f	0.00000	0.99375	0.25355	m(x)	1.0	0.0486
O3	16 g	0.21590	0.37662	0.00405	1	1.0	0.0058

Space Group: *C*mca (64); a= 6.084(5) Å; b=11.500(8)Å; c=8.289(6)Å ; α=β=γ= 90;Z=4; V=580.008(5)$Å^3$.

Reliability Factors: Rp = 2.49%, Rwp = 3.66%, $\chi 2$ = 5.76.

Bond Lengths (Å): Zn1/Ni1-O : 2.1515Å (Avg.); Zn2-O:2.2037Å (Avg.); V-O: 1.6499Å (Avg.).

Δ= 1.2466 [Zn2/Ni1]; Δ= 0.80 [Zn1].

Δ is the polyhedral distortion parameter defined by $\Delta = 1/N \sum [\{(r_i - r)/r\}^2]10^3$; where N is the number of bonds and r_i and r are individual and average bond lengths, respectively.

Rietveld refinement for Cu^{2+} substituted vanadate compound

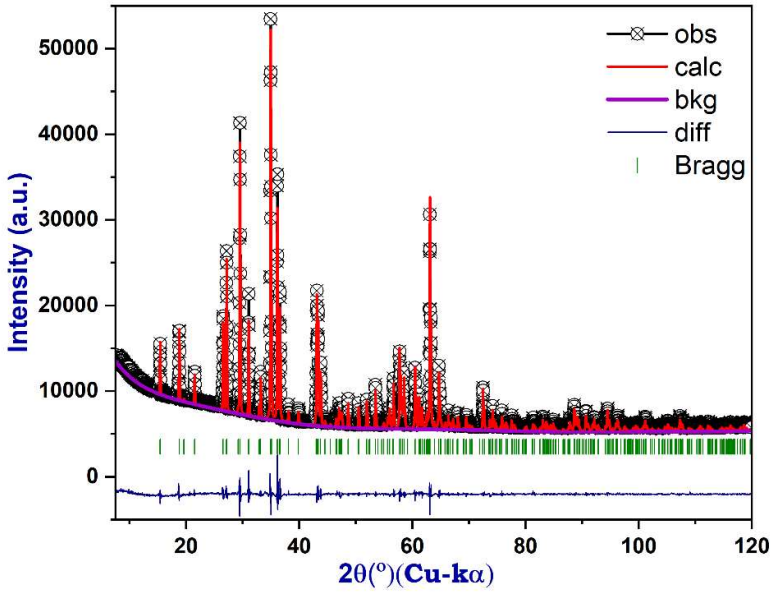

Crystallographic parameters for $(Cu_{0.4}Zn_{2.6})V_2O_8$ compound generated from the Rietveld refinement of the PXRD data.

Atom	Wyck. Symbol	x/a	y/b	z/c	Site Sym	Frac	U [Å²]
Zn2/Cu1	8 e	0.25000	0.13662	0.25000	2(y)	0.734/0.266	0.0066
Zn1	4 a	0.0	0.0	0.0	2/m(x)	1	0.0158
V1	8 f	0.00000	0.37810	0.12346	m(x)	1.0	0.0028
O1	8 f	0.00000	0.25332	0.22793	m(x)	1.0	0.0173
O2	8 f	0.00000	0.99450	0.24976	m(x)	1.0	0.0269
O3	16 g	0.22111	0.37488	0.01251	1	1.0	0.0107

Space Group: *C*mca (64); a= 6.12158(5) Å; b=11.52732(9)Å; c=8.27498(6)Å ; α=β=γ= 90;Z=4; V=583.928(5)$Å^3$.

Reliability Factors: Rp = 3.15%, Rwp = 5.80%, $\chi 2$ =4.250 .

Bond Lengths (Å): Zn1/Cu1-O : 2.1570Å (Avg.); Zn2-O:2.1807Å (Avg.); V-O: 1.6633Å (Avg.).

Δ= 1.454 [Zn2/Cu1]; Δ= 1.266[Zn1].

Δ is the polyhedral distortion parameter defined by $\Delta = 1/N \sum [\{(r_i - r)/r\}^2]10^3$; where N is the number of bonds and r_i and r are individual and average bond lengths, respectively.

Figure S3. Rietveld refinement and Crystallographic parameters generated from the Rietveld refinement for of $Zn_{3-x}M_xV_2O_8$ (M= Co, Ni, Cu). Observed (o), calculated (red line) and difference (bottom blue line) profiles are shown. The vertical bars indicate Bragg reflections (|).

Tanabe Sugano and orgel diagram for doped transition metal ion

The ground state in an octahedral environment of Co^{2+} is $^4T_{1g}$. There are three transitions observed. (i) $^4T_{1g} \rightarrow {}^4T_{2g}(F)$ transitions falls in the IR region, $^4T_{1g} \rightarrow {}^4A_{2g}(F)$ and $^4T_{1g} \rightarrow {}^4T_{1g}(P)$ transition fall in the visible region. The octahedra Ni^{2+} ion (d^8) has the ground state of $^3A_{2g}$. There are three transitions observed, (i) $^3A_{2g}(F) \rightarrow {}^3T_{2g}(F)$ observed in the IR region, (ii) $^3A_{2g} \rightarrow {}^3T_{1g}(F)$ and (iii) $^3A_{2g} \rightarrow {}^3T_{1g}(P)$ both transitions observed in the visible region. In this study, compounds have distorted Co^{2+}/Ni^{2+} octahedra. Due to this distortion, forbidden transitions become allowed, which results in the splitting of the transitions. When the energy of the allowed transitions is comparable with forbidden transitions, we observe shoulder peaks along with allowed transitions. The octahedral Cu^{2+} ions (d^9) have the ground state ^2E_g, it is subject to considerable Jahn-Teller distortion. There is only one transition ($^2Eg \rightarrow {}^2T_{2g}$) observed in the visible region.

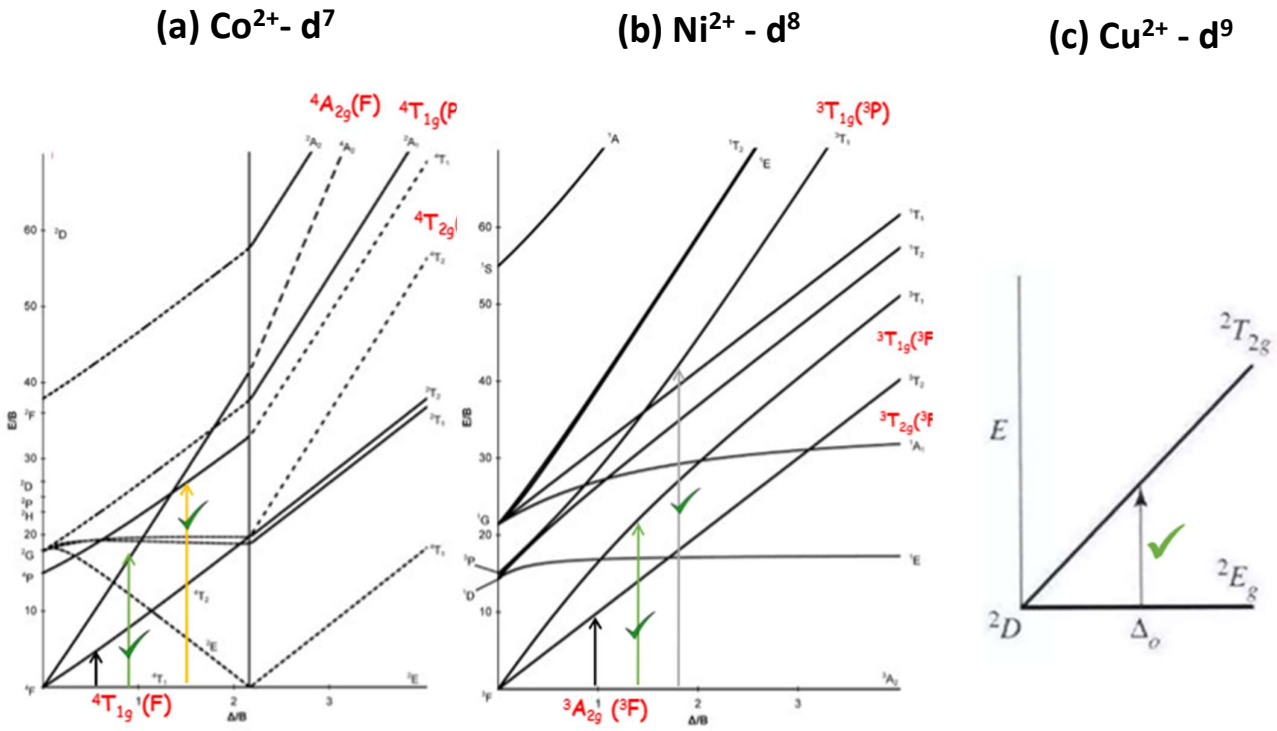

Figure S4: Tanabe–Sugano diagrams of (a) d^7 (b) d^8 and orgel diagram of d^9 configurations, figures show green colored arrows indicating the allowed transitions. The octahedral energy term mentioned here.

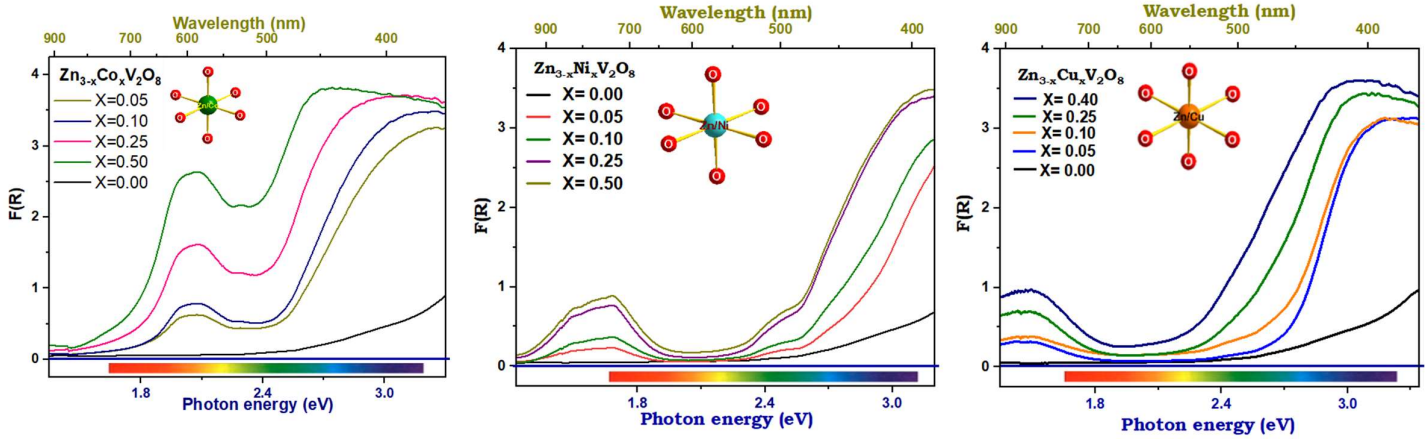

Figure S5: Optical absorption (UV/Vis) spectra of $Zn_{3-x}M_xV_2O_8$ (M= Co, Ni, Cu) prepared vanadate compounds.

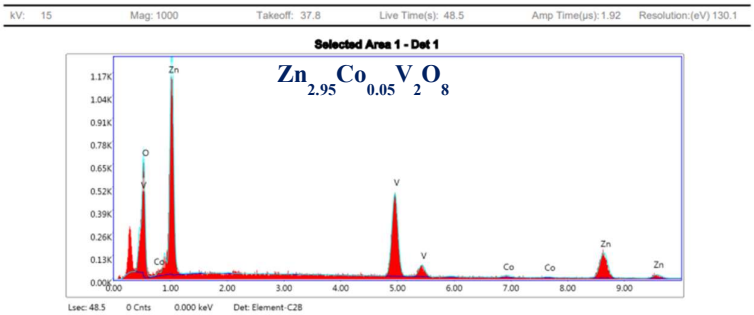

Element	Atomic Weight	Weight Percentage (Calculated)	Weight Percentage/ atomic weight	Atomic Percentage (Calculated)	Weight Percentage (observed)	Atomic Percentage (observed)
O K	15.99	30.05	1.879	61.56	13.84	37.21
Zn L	65.38	45.31	0.693	22.70	52.40	34.48
V K	50.94	23.93	0.469	15.36	32.05	27.06
Co K	58.93	0.69	0.011	0.36	1.71	1.25
Total	**425.61**	100	**3.052**	**100**		

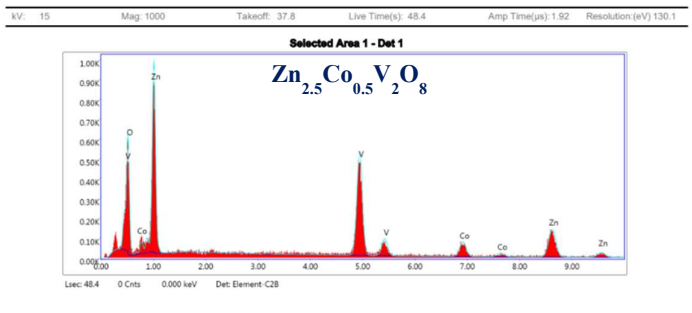

Element	Atomic Weight	Weight Percentage (Calculated)	Weight Percentage/ atomic weight	Atomic Percentage (Calculated)	Weight Percentage (Observed)	Atomic Percentage (Observed)
O K	15.99	30.26	1.892	61.54	12.24	33.64
Zn L	65.38	38.66	0.591	19.22	43.00	28.93
V K	50.94	24.10	0.473	15.38	34.42	29.71
Co K	58.93	06.97	0.118	03.83	10.34	7.72
Total	**422.715**	**100**	**3.074**	**100**		

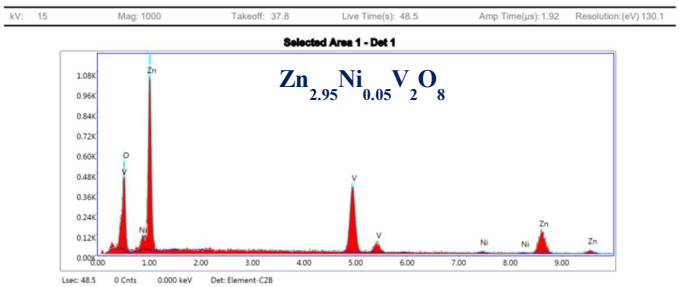

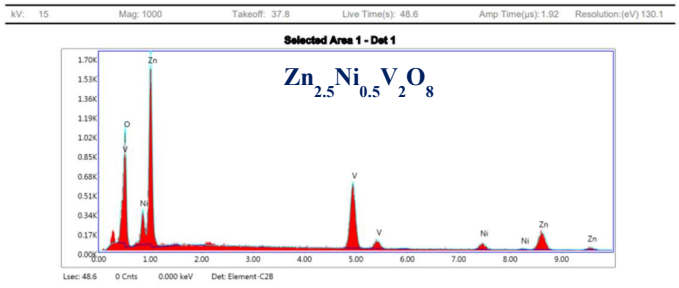

Element	Atomic Weight	Weight Percentage (Calculated)	Weight Percentage/ atomic weight	Atomic Percentage (Calculated)	Weight Percentage (Observed)	Atomic Percentage (Observed)
O K	15.99	30.05	1.879	61.56	12.83	35.24
Zn L	65.38	45.31	0.693	22.70	53.64	36.05
V K	50.94	23.93	0.469	15.36	31.72	27.35
Ni K	58.69	0.68	0.011	0.36	1.81	1.35
Total	425.60	100	3.052	100		

Element	Atomic Weight	Weight Percentage (Calculated)	Weight Percentage (Calc)/ Atomic weight	Atomic Percentage (Calculated)	Weight Percentage (Observed)	Atomic Percentage (Observed)
O K	15.99	30.27	1.893	61.56	15.57	40.33
Zn L	65.38	38.67	0.591	19.21	45.57	28.88
V K	50.94	24.10	0.473	15.38	31.39	25.53
Ni K	58.69	06.94	0.118	03.83	7.47	5.27
Total	422.59	100	3.075	100		

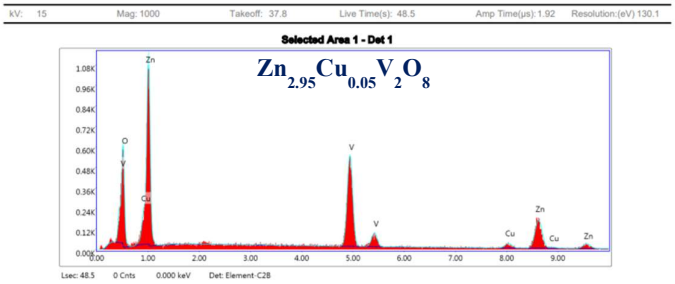

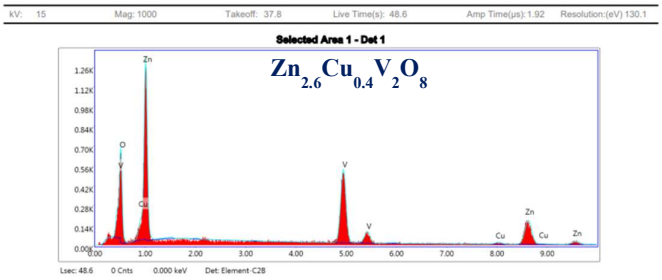

Element	Atomic Weight	Weight Percentage (Calculated)	Weight Percentage (Calc)/ Atomic weight	Atomic Percentage (Calculated)	Weight Percentage (Observed)	Atomic Percentage (Observed)
O K	15.99	30.04	1.878	61.55	13.26	36.02
Zn L	65.38	44.53	0.681	22.32	50.29	33.43
V K	50.94	23.93	0.469	15.37	33.33	28.42
Cu K	63.54	01.49	0.023	00.75	3.11	2.13
Total	425.75	100	3.051	100		

Element	Atomic Weight	Weight Percentage (Calculated)	Weight Percentage (Calc)/ Atomic weight	Atomic Percentage (Calculated)	Weight Percentage (Observed)	Atomic Percentage (Observed)
O K	15.99	30.06	1.879	61.50	11.87	33.03
Zn L	65.38	42.25	0.646	21.14	46.32	31.55
V K	50.94	23.94	0.469	15.35	35.25	30.82
Cu K	63.54	3.73	0.058	01.89	6.57	4.60
Total	425.48	100	3.055	100		

Figure S6: SEM-EDX spectra of $Zn_{3-x}M_xV_2O_8$(M= Co, Ni, Cu).

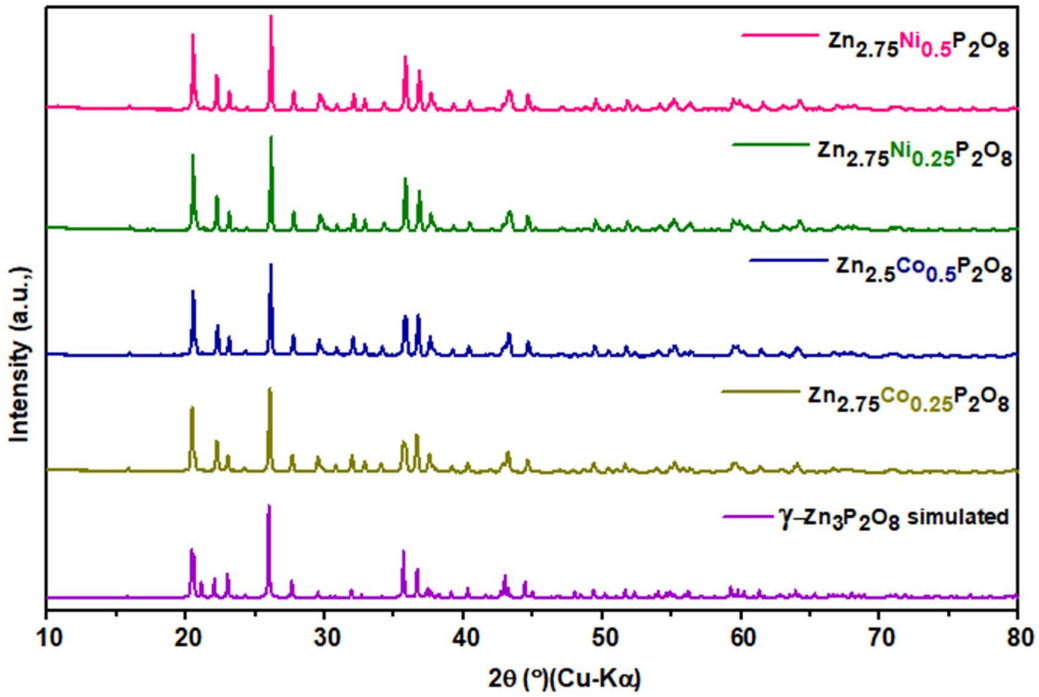

Figure S7: PXRD patterns of $Zn_{3-X}M_xP_2O_8$ (M= Co, Ni) prepared Phosphate compounds.

Rietveld refinement for Co^{2+} substituted phosphate compound

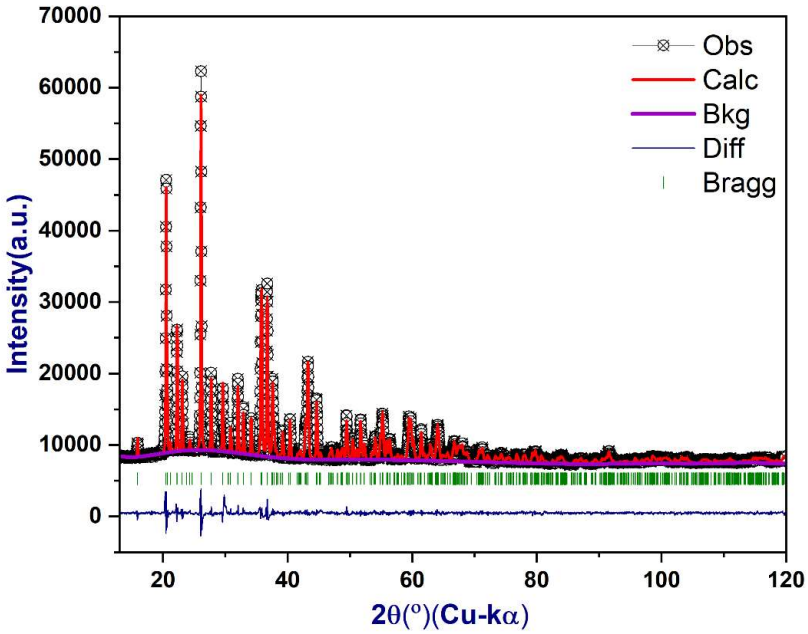

Crystallographic parameters for $(Co_{0.5}Zn_{2.5})P_2O_8$ compound generated from the Rietveld refinement of the PXRD data.

Atom	Wyck. Symbol	x/a	y/b	z/c	Site Sym	Frac	U [Å²]
Co1/Zn1	2 b	0.00000	0.00000	0.50000	-1	0.39/0.61	0.0035
Co2/Zn2	4 e	0.62024	0.13867	0.07760	1	0.11/0.89	0.0063
P1	4 e	0.19415	0.19092	0.04063	1	1.000	0.0049
O1	4 e	0.05050	0.13916	0.85054	1	1.000	0.0111
O2	4 e	0.13586	0.20125	0.327245	1	1.000	0.0150
O3	4 e	0.24626	0.36580	0.934516	1	1.000	0.0078
O4	4 e	0.35595	0.07686	0.049800	1	1.000	0.0386

Space Group: $P12_1/n1$ (14); a= 7.53338(24) Å; b= 8.43676(14) Å; c= 5.04085(13) Å; α=γ= 90;β= 95.0473(15); Z=2; V= 319.141(6)$Å^3$.

Reliability Factors: Rp =1.36%, Rwp = 2.20%, $\chi 2$ =4.43 .

Bond Lengths (Å): Zn1/Co1- O : 2.1834Å (Avg.); Zn2/Co2-O:2.0444Å (Avg.); P-O: 1.5442Å (Avg.).

Δ= 0.338 [Zn1/Co1]; Δ=8.8958 [Zn2/Co2]

Δ is the polyhedral distortion parameter defined by $\Delta = 1/N \sum [\{(r_i - r)/r\}^2]10^3$; where N is the number of bonds and r_i and r are individual and average bond lengths, respectively

Rietveld refinement for Ni^{2+} substituted phosphate compound

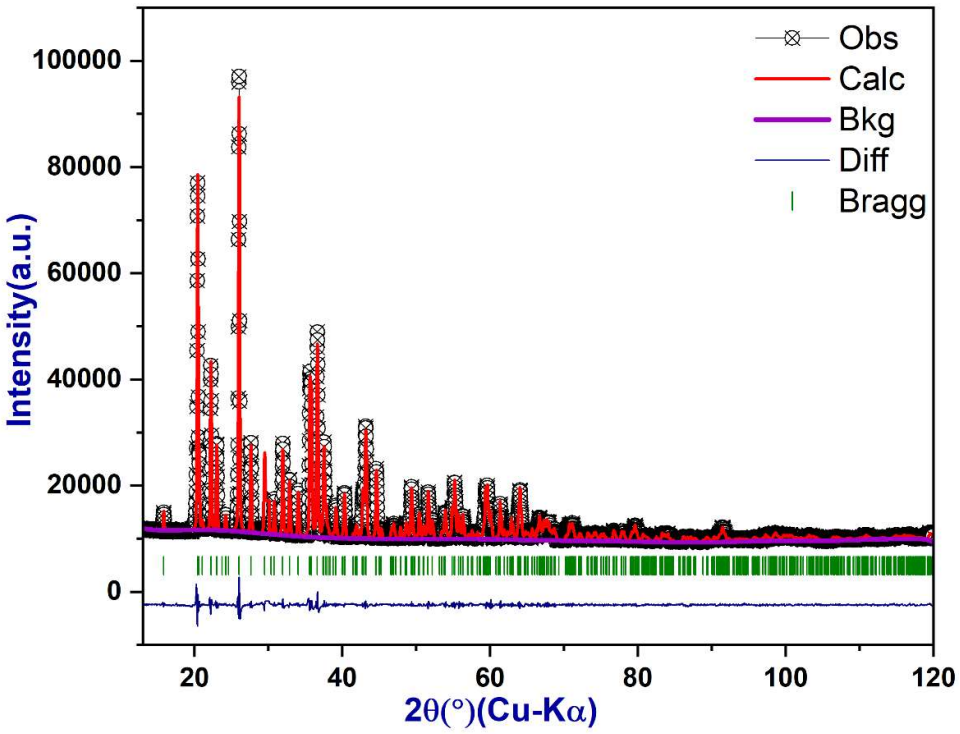

Crystallographic parameters for $(Ni_{0.5}Zn_{2.5})P_2O_8$ compound generated from the Rietveld refinement of the PXRD data.

Atom	Wyck. Symbol	x/a	y/b	z/c	Site Sym	Frac	U [Å²]
Ni1/Zn1	2 b	0.00000	0.00000	0.50000	-1	0.39/0.61	0.0250
Ni2/Zn2	4 e	0.61715	0.13479	0.07760	1	0.11/0.89	0.0259
P1	4 e	0.20206	0.19600	0.03880	1	1.000	0.0204
O1	4 e	0.05543	0.13365	0.82171	1	1.000	0.0413
O2	4 e	0.12569	0.20184	0.30583	1	1.000	0.0289
O3	4 e	0.24826	0.36451	0.93462	1	1.000	0.0307
O4	4 e	0.35511	0.06685	0.03490	1	1.000	0.0447

Space Group: $P12_1/n1$ (14); a= 7.53179(18) Å; b= 8.44593(10) Å; c= 5.03805(10) Å; α=γ= 90°;β= 95.1654(11);Z=2;

V= 319.184(5)$Å^3$.

Reliability Factors: Rp =1.76%, Rwp = 2.59%, $\chi 2$ =5.56 .

Bond Lengths (Å): Zn1/Ni1-O : 2.1405Å (Avg.); Zn2/Ni2-O:2.032Å (Avg.); P-O: 1.5598Å (Avg.).

Δ= 1.06 [Zn1/Ni1]; Δ=2.94 [Zn2/Ni2]

Δ is the polyhedral distortion parameter defined by $\Delta = 1/N \sum [\{(r_i - r)/r\}^2]10^3$; where N is the number of bonds

Figure S8. Rietveld refinement of $Zn_{3-x}M_xP_2O_8$ (M=Co, Ni). Observed (o), calculated (red line) and difference (bottom blue line) profiles are shown. The vertical bars indicate Bragg reflections (|).

Crystallographic information: (γ-$Zn_3P_2O_8$): $Zn_2MgP_2O_8$

Crystal system	Monoclinic
Space group	*P* 1 2_1/n 1 (14)
Unit cell dimensions	a=7.569(1)Å; b=8.355(1)Å; c=5.059(1)Å; β=94.95(1)°
Cell volume	318.73 Å^3
Z	2

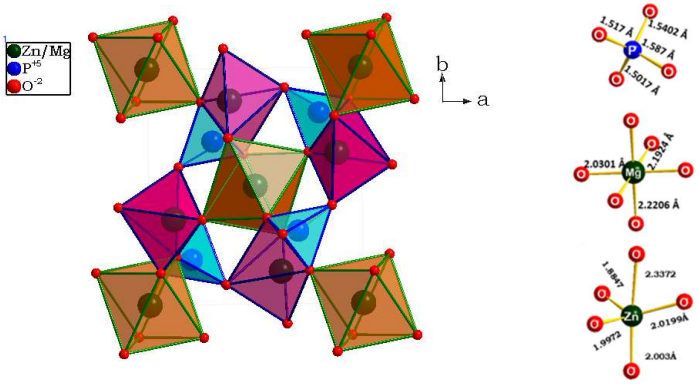

Atom	Oxidation state	Wyck symbol	X	Y	Z	SOF
Zn	+2	4 e	0.616(1)	0.138(1)	0.086(1)	0.88
Mg	+2	4 e	0.616(1)	0.138(1)	0.086(1)	0.12
Zn	+2	2 b	0	0	0.5	0.24
Mg	+2	2 b	0	0	0.5	0.76
P	+5	4 e	0.198(1)	0.191(1)	0.036(1)	1
O	-2	4 e	0.053(2)	0.135(1)	0.831(3)	1
O	-2	4 e	0.125(3)	0.205(2)	0.320(4)	1
O	-2	4 e	0.250(2)	0.360(2)	0.949(4)	1
O	-2	4 e	0.358(2)	0.084(2)	0.055(3)	1

Figure S9: The crystal structure and crystallographic information of $Zn_2MgP_2O_8$ (γ-$Zn_3P_2O_8$).

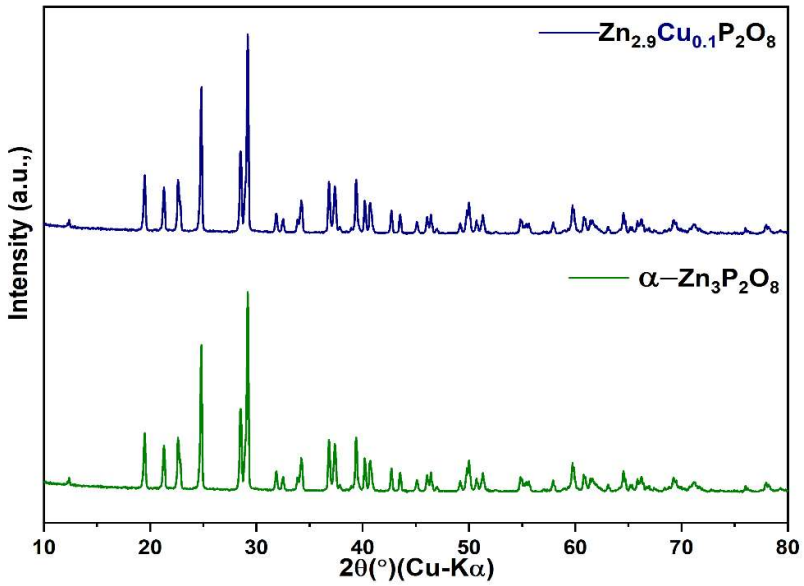

Figure S10: PXRD patterns of $Zn_{3-X}M_xP_2O_8$ (M= Cu) prepared Phosphate compound.

Crystallographic information: α-$Zn_3P_2O_8$

Crystal system	Monoclinic
Space group	*C* 1 2/c 1 (15)
Unit cell dimensions	a=8.14(2)Å; b=5.63(1)Å; c=15.04(4)Å; β=105.13(8)°
Cell volume	665.36 Å^3
Z	4

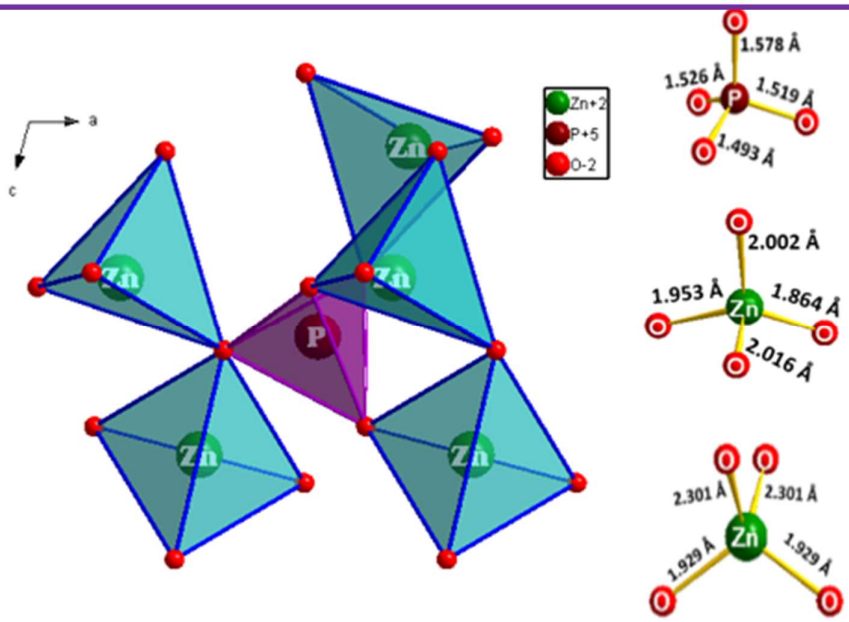

Atom	Oxidation state	Wyck symbol	X	Y	Z	SOF
Zn	+2	4 e	0	0.7448(9)	0.25	1
Zn	+2	8 f	0.2678(2)	0.5548(7)	0.0675(1)	1
P	+5	8 f	0.1592(4)	0.0634(14)	0.1286(2)	1
O	-2	8 f	0.2929(14)	0.0607(39)	0.2211(8)	1
O	-2	8 f	0.1197(16)	0.3092(43)	0.0770(8)	1
O	-2	8 f	0.2129(14)	0.9021(14)	0.0625(7)	1
O	-2	8 f	0.9935(13)	0.9676(33)	0.1429(6)	1

Figure S11. Crystal structure and crystallographic information of α-$Zn_3P_2O_8$.

Color of the doped sample under day light

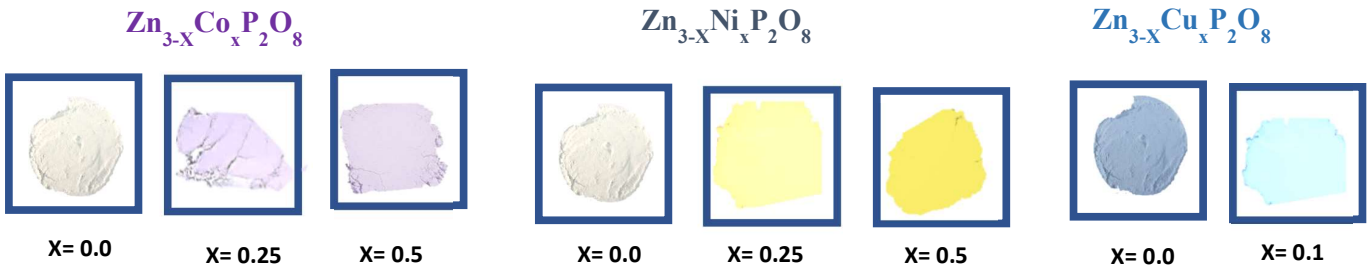

Figure S12. Color of $Zn_{3-x}M_xP_2O_8$ (M= Co, Ni, Cu) powder samples under day light.

Correlation diagram for Co^{2+} with different symmetries

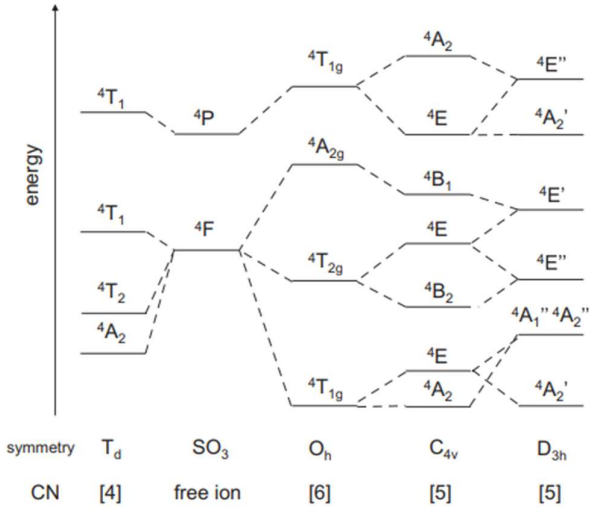

Figure S13. Correlation diagram for Co^{2+} with symmetries C_{4v}, D_{3h} (Co), T_d (Co) and O_h (Co). (CN: coordination number).[8]

Tanabe Sugano diagram for trigonal bipyramidal geometry of Co^{2+} and Ni^{2+} ions.

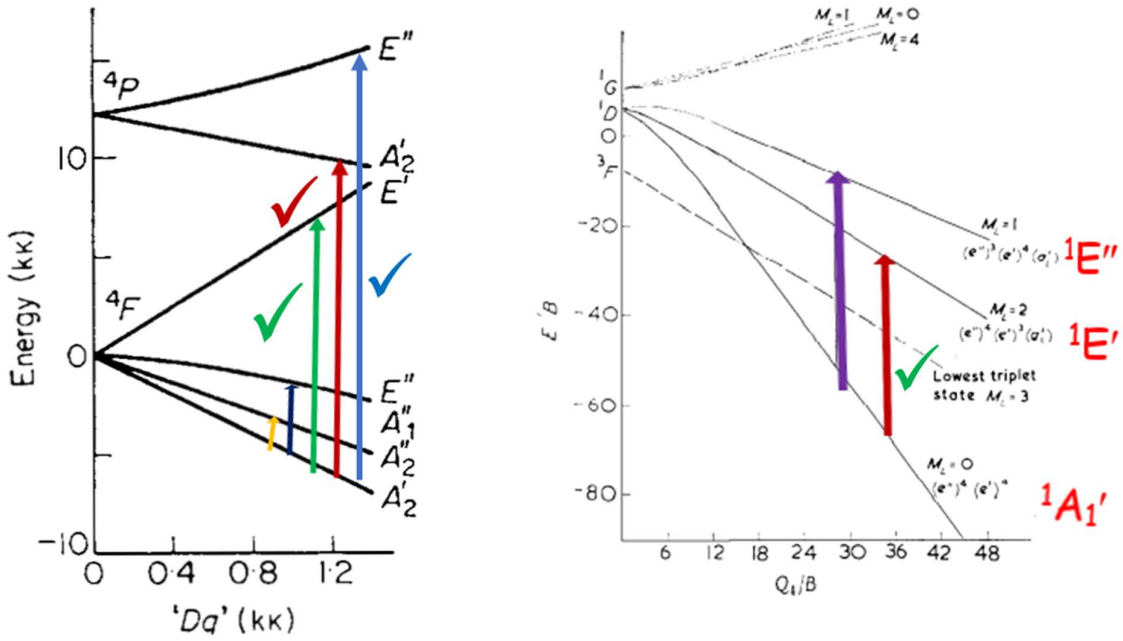

The Co^{2+} in trigonal bipyramidal environment, there are four bands observed. The absorption transitions, $^4A'_2(F) \rightarrow {}^4E''(F)$ and $^4A'_2(F) \rightarrow {}^4E'(F)$ fall in the IR region. The transitions $^4A'_2(F) \rightarrow {}^4A'_2(P)$ and $^4A'_2(F) \rightarrow {}^4E''(P)$. The transitions to the $^4A_2$ and $^4E''$ levels, though vibronically allowed, are electronically forbidden. The Ni^{2+} in trigonal bipyramidal environment[9], The ground state configuration $(e'')^4(e')^4$ belongs to $^1A'_1$. Two Spin-singlet excited state can be derived by single electron excitation;1. $(e'')^4(e')^3(a_1')$ belongs to $^1E'$ and 2. $(e'')^4(e')^3(a_1')$ belongs to $^1E''$.

Figure S14: Tanabe Sugano diagram for trigonal bipyramidal geometry of Co^{2+} and Ni^{2+} ions.

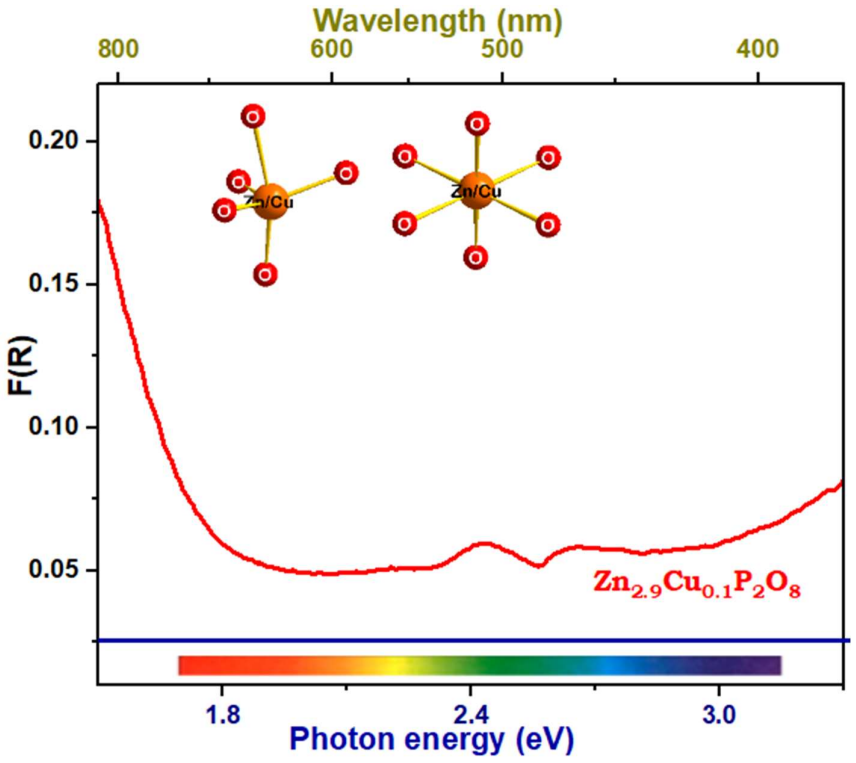

Figure S15: Optical absorption (UV/Vis) spectra of the $Zn_{3-x}Cu_xP_2O_8$ ($0 < x \leq 0.1$)

SEM-EDS spectrum of doped sample

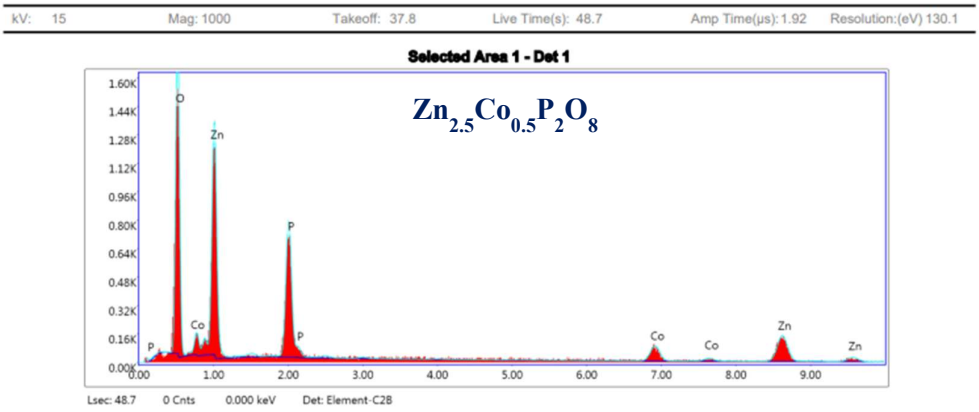

Element	Atomic Weight	Weight Percentage (Calculated)	Weight Percentage/ atomic weight	Atomic Percentage (Calculated)	Weight Percentage (observed)	Atomic Percentage (observed)
O K	15.99	33.41	2.089	61.54	26.86	54.76
Zn K	65.38	42.70	0.653	19.23	47.90	23.90
P K	30.97	16.18	0.522	15.38	14.75	15.53
Co K	58.93	07.69	0.130	03.83	10.49	5.81
Total	**382.77**	**100**	**3.394**	**100**		

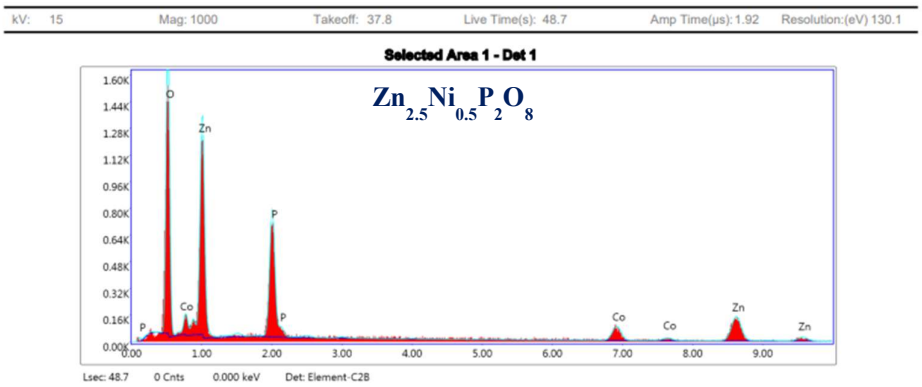

Element	Atomic Weight	Weight Percentage (Calculated)	Weight Percentage/ atomic weight	Atomic Percentage (Calculated)	Weight Percentage (observed)	Atomic Percentage (observed)
O K	15.99	33.42	2.090	61.56	29.66	57.96
Zn K	65.38	42.71	0.653	19.23	47.28	22.62
P K	30.97	16.18	0.522	15.37	14.97	15.11
Ni K	58.69	07.66	0.130	03.82	8.09	4.31
Total	**382.66**	**100**	**3.395**	**100**		

Figure S16. SEM-EDX spectra of $Zn_{3-x}M_xP_2O_8$(M=Co,Ni)

Crystallographic information: Co_2TiO_4 Vs Co_2SnO_4

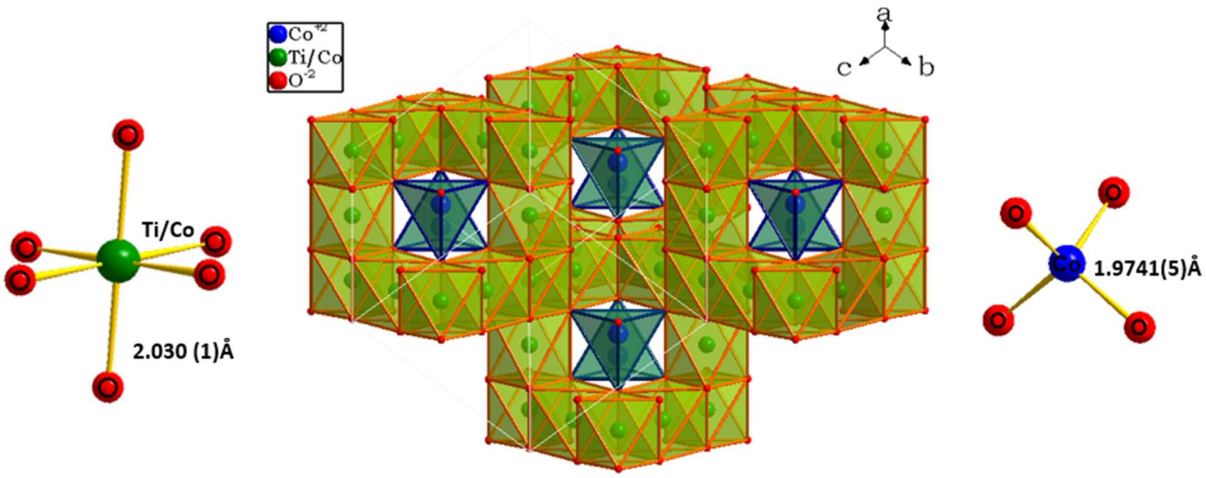

Co_2TiO_4

Crystal system	Cubic
Space group	*F* d -3 m (227)
Unit cell dimensions	*a* = 8.4440(4) Å
Cell volume	602.07 Å^3
Z	8

Atom	Oxidation state	Wyck symbol	X	SOF
Co	+2	8 b	0.375	1
Co	+2	16 c	0	0.5
Ti	+4	16 c	0	0.5
O	-2	32 e	0.24002(11)	1

Co_2SnO_4

Crystal system	Cubic
Space group	*F* d -3 m (227)
Unit cell dimensions	*a* = 8.636 Å
Cell volume	644.08 Å^3
Z	8

Atom	Oxidation state	Wyck symbol	X	SOF
Co	+2	8 a	0	1
Co	+2	16 d	0.625	0.5
Sn	+4	16 d	0.625	0.5
O	-2	32 e	0.383	1

Figure S17. Crystal structure and crystallographic information of Co_2TiO_4 and Co_2SnO_4.

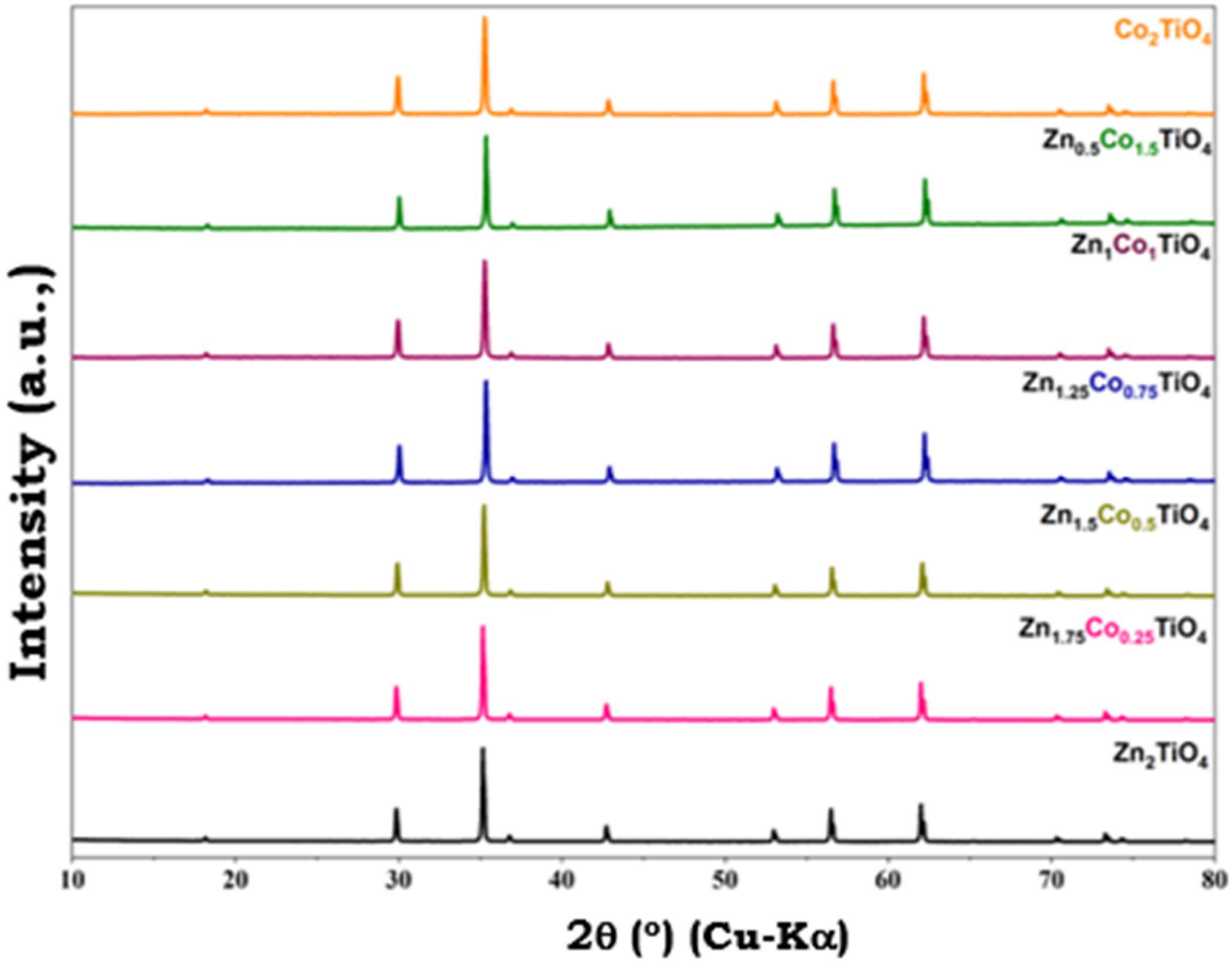

Figure S18. The PXRD Pattern of $Zn_{2-x}Co_xTiO_4$ (x= 0.0 to 2.0) samples

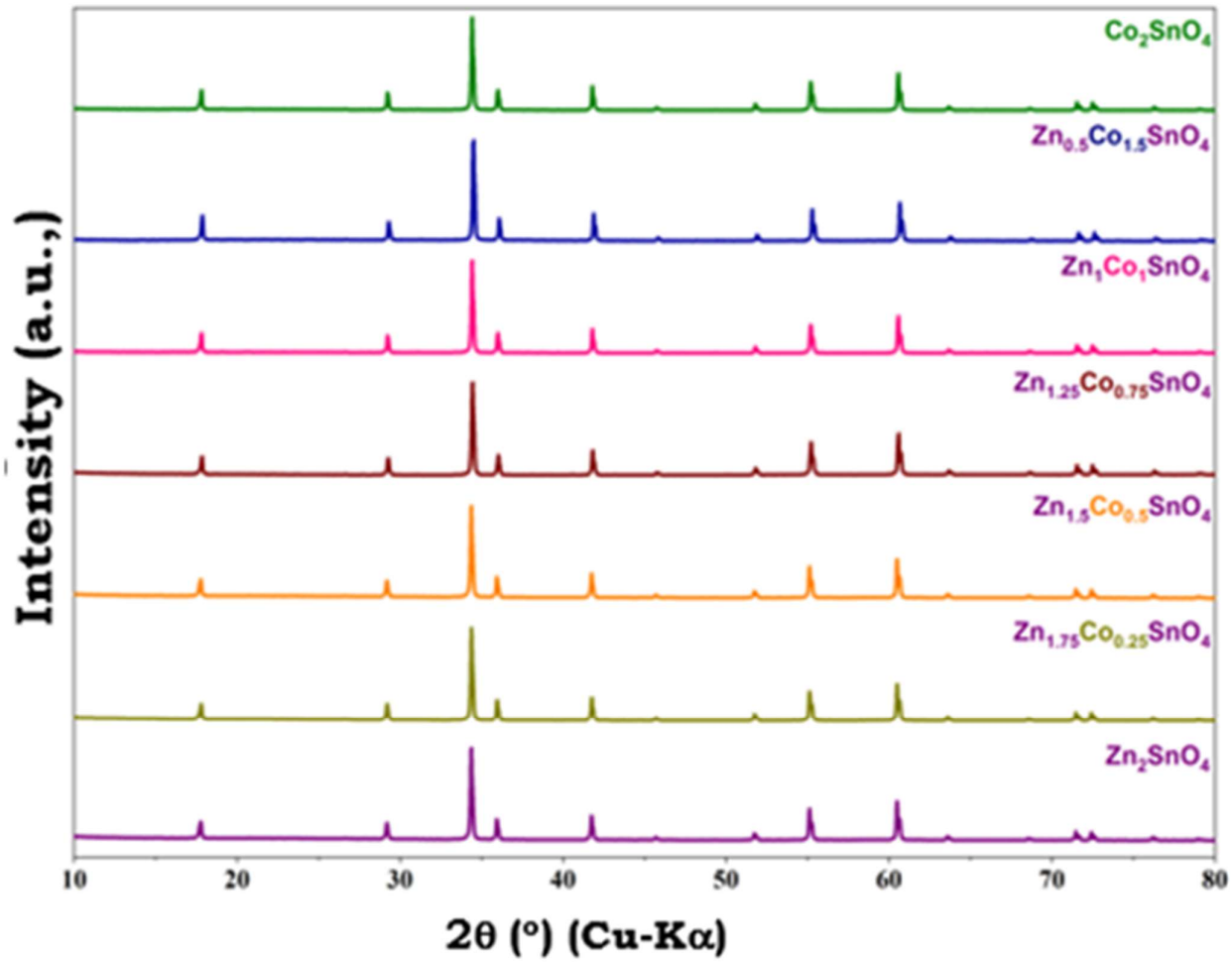

Figure S19. The PXRD Pattern of $Zn_{2-x}Co_xSnO_4$ (x= 0.0 to 2.0) samples

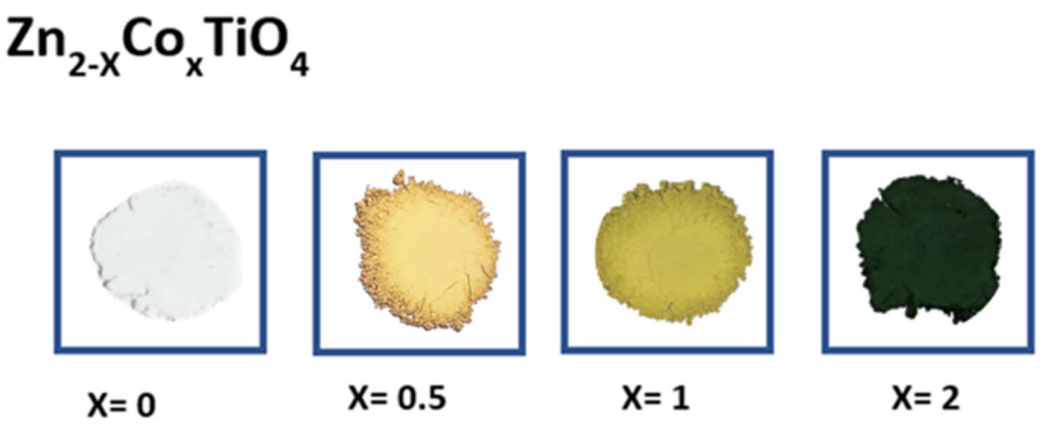

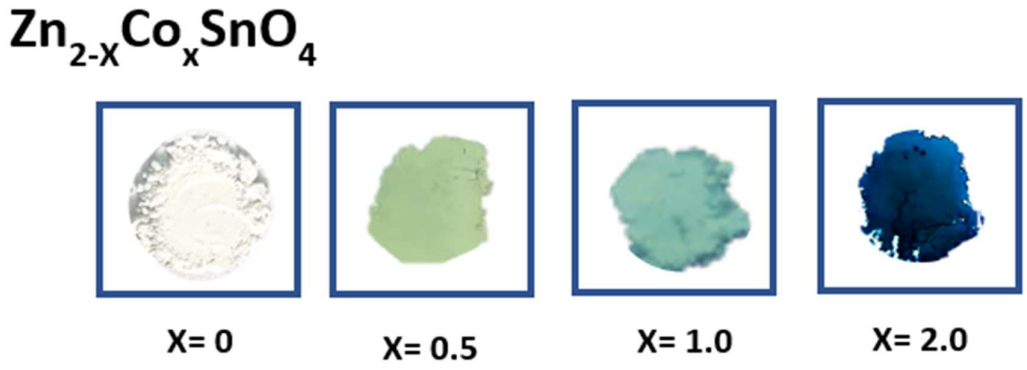

Figure S20. The Color of $Zn_{2-x}Co_xAO_4$ (A=Ti, Sn) powder samples under day light.

Orgel and Tanabe Sugano diagram for Co^{2+} ion

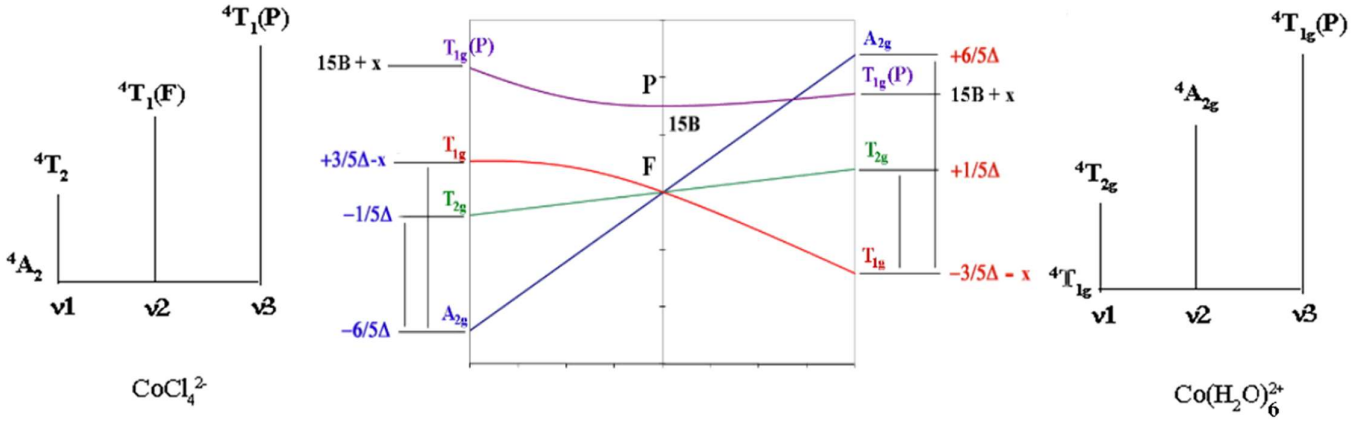

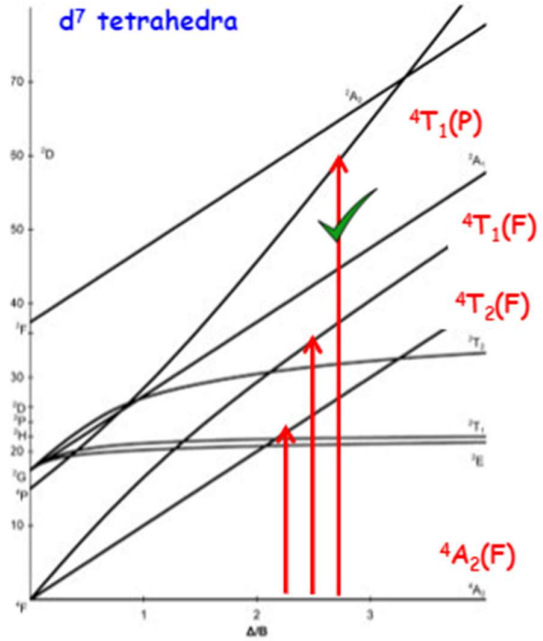

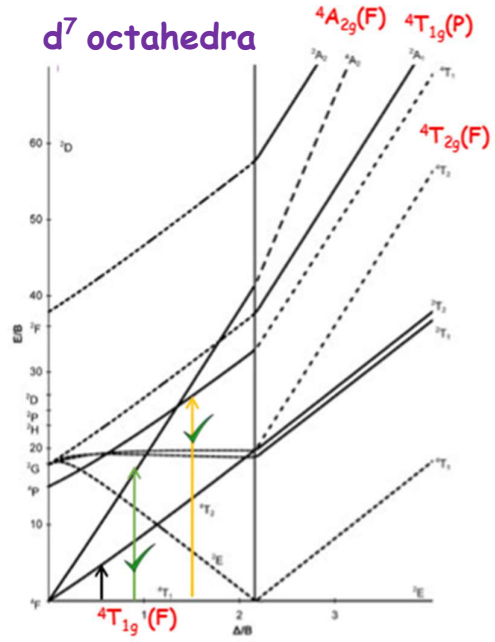

Figure S21. Orgel and Tanabe Sugano diagram for Co^{2+} ion in both octahedral and tetrahedral geometry. The figures show green colored arrows indicating the allowed transitions[10].

NIR Reflectivity

TiO_2 is a white pigment having a strong NIR reflectance. The light-yellow colored compound, $Zn_3V_2O_8$ displays NIR reflectivity of around 80% which is exhibiting slightly better NIR reflectivity as compared to TiO_2. The beige yellow color compound, **$Zn_{1.95}Ni_{0.05}V_2O_8$, $Zn_{1.75}Ni_{0.25}V_2O_8$, $Zn_{1.9}Ni_{0.1}V_2O_8$, $Zn_{1.75}Co_{0.25}V_2O_8$, $Zn_{1.95}Co_{0.05}V_2O_8$** shows NIR reflectivity of around 85% which is comparable to that of TiO_2. Therefore, the newly synthesized transition metal substituted $Zn_3V_2O_8$ could be good candidates as white pigments with high NIR reflectivity.

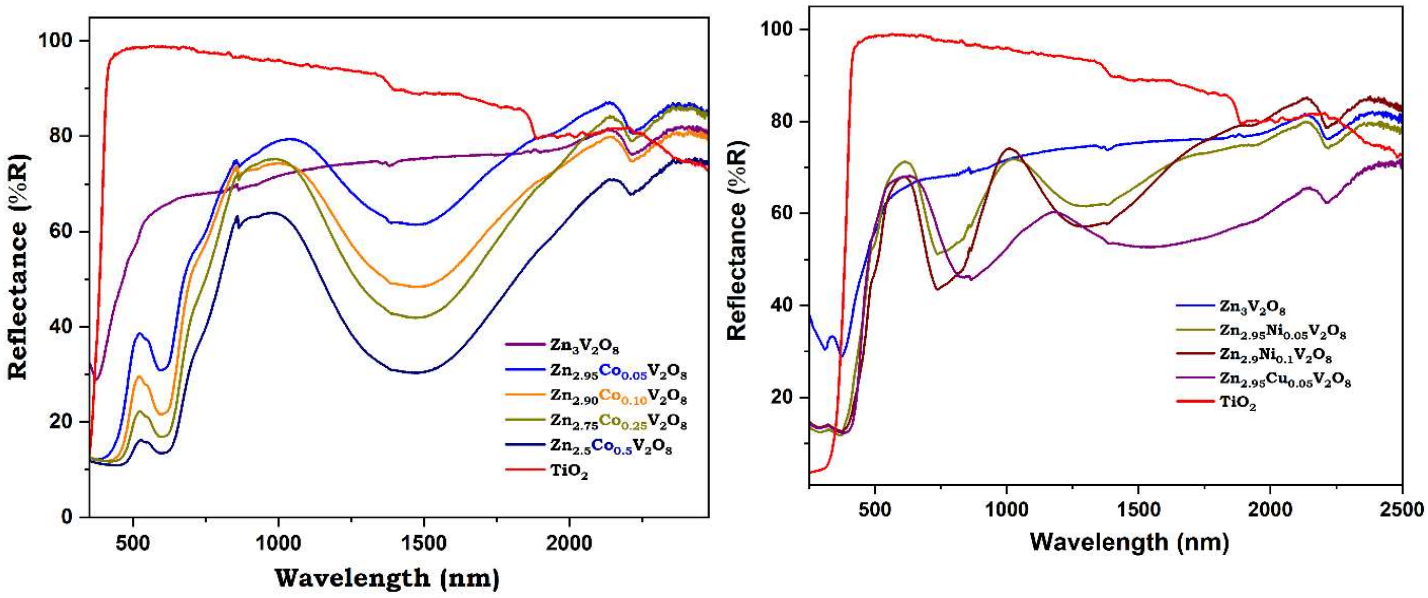

Figure S22. NIR reflectivity of $Zn_{3-x}M_xV_2O_8$(M= Co, Ni, Cu)

The white colored compound, $Zn_3P_2O_8$ displays NIR reflectivity of around 75% which is exhibiting slightly better NIR reflectivity as compared to TiO_2. The following color compound, $Zn_{2.95}Ni_{0.5}P_2O_8$, $Zn_{2.75}Ni_{0.25}P_2O_8$, shows NIR reflectivity of around 70% which is comparable to that of TiO_2. Therefore, the newly synthesized transition metal substituted $Zn_3P_2O_8$ could be good candidates as white pigments with high NIR reflectivity.

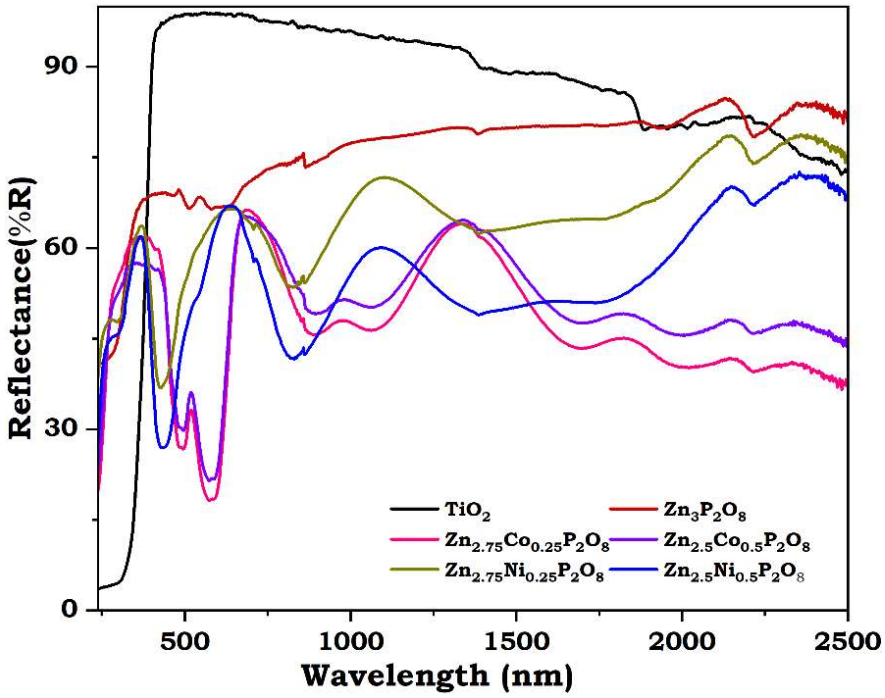

Figure S23. NIR reflectivity of $Zn_{3-x}M_xP_2O_8$(M= Co, Ni, Cu)

CIE 1931 Diagram and color coordinates

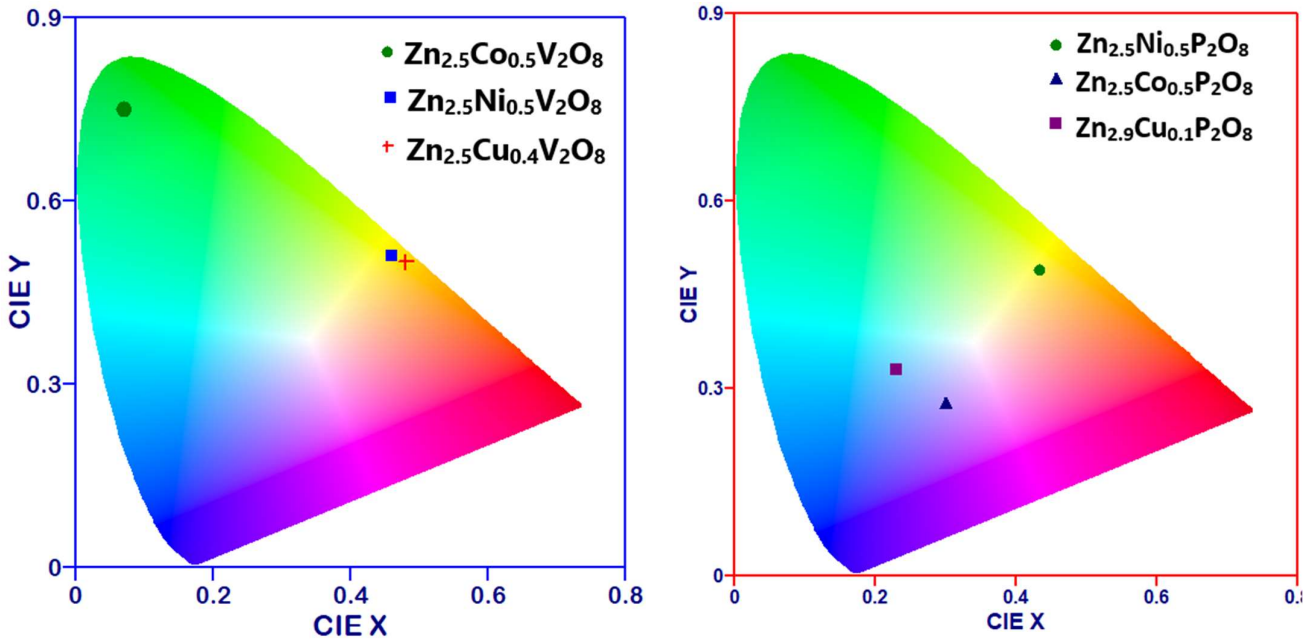

Compound	CIE X	CIE Y	L*	a*	b*
$Zn_{2.5}Co_{0.5}V_2O_8$	0.07	0.75	45.39	-4.84	08.95
$Zn_{2.5}Ni_{0.5}V_2O_8$	0.46	0.51	78.17	-3.26	43.00
$Zn_{2.6}Cu_{0.4}V_2O_8$	0.48	0.50	68.34	3.52	39.18

Compound	CIE X	CIE Y	L*	a*	b*
$Zn_{2.5}Co_{0.5}P_2O_8$	0.29	0.27	66.95	12.28	-17.50
$Zn_{2.5}Ni_{0.5}P_2O_8$	0.37	0.38	79.21	1.14	27.98
$Zn_{2.9}Cu_{0.1}P_2O_8$	0.31	0.33	88.25	0.22	0.92

In order to quantify the color of the compounds further, we have determined the color coordinates from CIE (International Commission on Illumination) 1931 (x, y (Chromaticity coordinates); L* (Lightness), a* and b* (Color space) parameters) of the prepared compounds. CIE standard illuminant D65 used in colorimetric calculations requiring representative daylight.

Figure S24. CIE chromaticity diagram and CIE coordinates of $Zn_{3-x}M_xA_2O_8$(M= Co, Ni, Cu); (A=V, P).

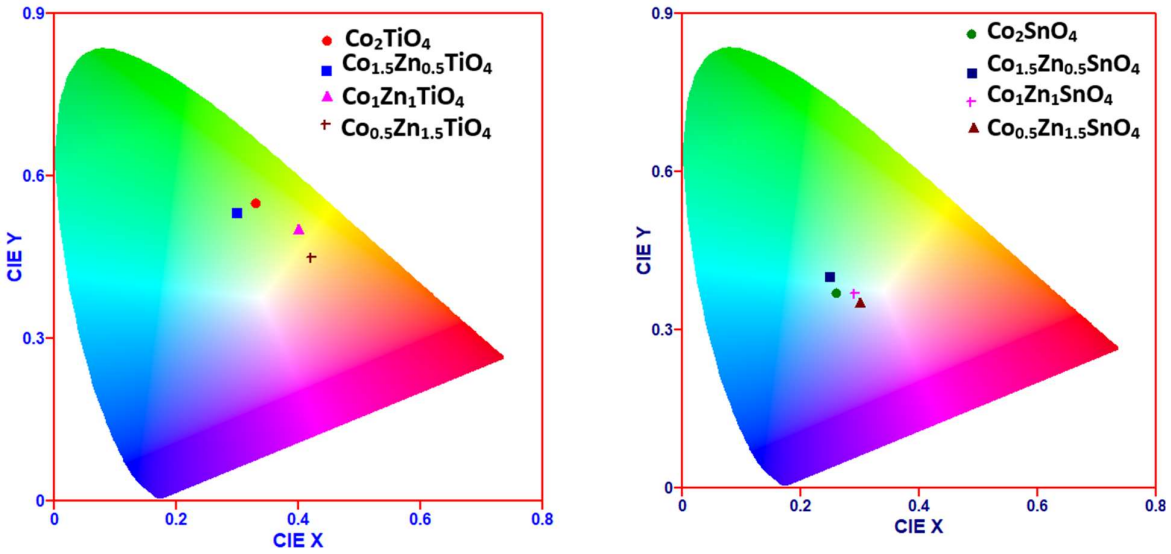

Compound	CIE X	CIE Y	L*	a*	b*
$Zn_{1.75}Co_{0.25}TiO_4$	0.368	0.387	71.17	0.12	25.00
$Zn_{1.75}Co_{0.5}TiO_4$	0.385	0.396	66.03	2.62	28.88
$Zn_{1.25}Co_{0.75}TiO_4$	0.385	0.394	60.25	3.16	26.17
$Zn_{1.0}Co_{1.0}TiO_4$	0.367	0.393	54.22	-1.92	21.41
$Zn_{0.5}Co_{1.5}TiO_4$	0.324	0.367	45.14	-6.48	08.75
Co_2TiO_4	0.340	0.310	40.67	-2.50	02.94
$Zn_{1.75}Co_{0.25}SnO_4$	0.315	0.343	74.97	-4.56	04.70
$Zn_{1.75}Co_{0.5}SnO_4$	0.310	0.344	69.67	-6.23	03.97
$Zn_{1.25}Co_{0.75}SnO_4$	0.300	0.339	63.74	-8.29	01.24
$Zn_{1.0}Co_{1.0}SnO_4$	0.290	0.337	59.03	-10.45	-0.69
$Zn_{0.5}Co_{1.5}SnO_4$	0.285	0.335	46.90	-9.79	-1.28
Co_2SnO_4	0.281	0.330	42.80	-9.03	-2.65

Figure S25. CIE chromaticity diagram and CIE coordinates of $Zn_{2-x}Co_xAO_4$ (A = Ti, Sn).

References:

1: B. H. Toby, *J. Appl. Crystallogr.* **2001**, *34*, 210.

2: R. A. Young, D. B. Wiles, *J. Appl. Crystallogr.* **1982**, *15*, 430.

3: B.J. Brinkworth, *Appl. Optics*. **1972**, *11*, 1434.

4. P. Makuła, M. Pacia, W. Macyk, *J. Phys. Chem. Lett*. **2018**, *9*, 6814– 6817.

5. K. R. J. Thomas, GoCIE V2, Department of Chemistry, Indian Institute of Technology Roorkee, India, **2009**.

6. A. D. Broadbent, *Color Res. Appl*. **2004**, 29, 267.

7. M. Abd Mutalib, M.A. Rahman, M.H.D Othman, A. F. Ismail, J. Jaafar, Scanning electron microscopy (SEM) and energy-dispersive X-ray (EDX) spectroscopy. *Membrane characterization*, **2017**, 161-179.

8. M. Hunault, J.-L. Robert, M. Newville, L. Galoisy, G. Calas, *Spectrochim. Acta Part A Mol. Biomol. Spectrosc*. **2014,***117*, 406– 12.

9. M. J. Norgett, J. H. M. Thornley, and L. M. Venanzi. *Coordination Chemistry Reviews* 2.1, **1967**, 83-98.

10. H.A.O. Hill, P. Day. Physical Methods in Advanced Inorganic Chemistry. John Wiley & Sons, Inc. **1968.**